A circular bioprocess for the sustainable conversion of polyethylene terephthalate to muconic acid with an engineered *Pseudomonas putida*

Pan Liu[a], Yi Zheng[a], Yingbo Yuan[a], Tong Zhang[a], Qingbin Li[a], Quanfeng Liang[a], Tianyuan Su[a, *], Qingsheng Qi[a, *]

[a]State Key Laboratory of Microbial Technology, Shandong University, Qingdao 266237, China.

[*]Corresponding authors:

Tel & Fax: +86-532-58632580; Email: qiqingsheng@sdu.edu.cn (Qingsheng Qi); sutianyuan@sdu.edu.cn (Tianyuan Su)

Electronic copy available at: https://ssrn.com/abstract=4110033

A circular bioprocess for the sustainable conversion of polyethylene terephthalate to muconic acid with an engineered *Pseudomonas putida*

Pan Liu[a], Yi Zheng[a], Yingbo Yuan[a], Tong Zhang[a], Qingbin Li[a], Quanfeng Liang[a], Tianyuan Su[a, *], Qingsheng Qi[a, *]

[a]State Key Laboratory of Microbial Technology, Shandong University, Qingdao 266237, China.

[*]Corresponding authors:

Tel & Fax: +86-532-58632580; Email: qiqingsheng@sdu.edu.cn (Qingsheng Qi); sutianyuan@sdu.edu.cn (Tianyuan Su)

Electronic copy available at: https://ssrn.com/abstract=4110033

Abstract

Many studies have highlighted the role of biosynthetic pathway for the valorization of polyethylene terephthalate (PET) waste. However, the existing chemical or enzymatic methods employ additional catalyst to degrade polymer before biotransformation of the degradation products, leading to the increase in process cost and complexity. In this study, we created a circular bioprocess for the sustainable upcycling of PET to high-value added product muconic acid (MA) with regeneration of biocatalyst. We constructed a multifunctional *Pseudomonas putida* KT2440 by metabolic engineering to simultaneously secret PET hydrolase LCC and synthesize MA from terephthalate in the same fermentation process. Ingeniously, MA and extracellular enzyme LCC can be separated from the fermentation fluid by ultrafiltration, and the latter was re-used for the next round of PET hydrolysis. Another PET hydrolysate ethylene glycol can support the cell growth during fermentation, which further improves the resource utilization of PET waste. 0.50 g MA was produced from 1 g PET in each cycle, reaching 68% of the theoretical conversion. This biological and circular process with the reproduced PET hydrolase should have advantageous over existing PET upcycling processes and may applied in the valorization of other plastics or biomass resources such as lignin.

Electronic copy available at: https://ssrn.com/abstract=4110033

Keywords: plastic upcycling, metabolic engineering, enzymatic hydrolysis, bioconversion, ultrafiltration

Electronic copy available at: https://ssrn.com/abstract=4110033

1. Introduction

Polyethylene terephthalate (PET) is one of the most commonly used plastics and widely exists in single-use beverage bottles, textiles and food packaging (Tsironi et al., 2022). However, post-consumer PET accumulated in the environment and unmanaged, resulting in serious environmental pollution and a significant loss of valuable resources (Kubowicz and Booth, 2017; Xu et al., 2021). Therefore, an innovative plastic recycling strategy is imperative to achieve the resourceful utilization of PET (Nikolaivits et al., 2021; Sardon and Li, 2020).

PET can be depolymerized to monomers and oligomers by physical and chemical methods, such as pyrolysis, ammonolysis, hydrolysis, methanolysis, and glycolysis (Barnard et al., 2021; Ghasemi et al., 2021; Ghosal and Nayak, 2022). Many chemo-bioprocesses have been developed to synthesize high-value chemicals from the monomers or oligomers after chemical or physical treatment of PET (Qi et al., 2021). PET pyrolysis under high temperature causes complete depolymerization into monomeric terephthalate (TPA) and ethylene glycol (EG) (Ikenaga et al., 2016; Yoshioka et al., 2004). Using PET pyrolysis products as the feedstock, Kenny et al. synthesized bioplastic polyhydroxyalkanoates (PHA) employed *Pseudomonas* strains isolated from PET-exposed soil (Kenny et al., 2008), and Kim et al. engineered

Electronic copy available at: https://ssrn.com/abstract=4110033

Escherichia coli and *Gluconobacter oxydans* to synthesize higher-value products such as gallic acid, pyrogallol, muconic acid (MA), vanillic acid and glycolate (Kim et al., 2019). PET ammonolysis is generally carried out with ammonium hydroxide at 70-180 °C, producing bis(2-hydroxyethyl) terephthalate (BHET), mono(hydroxyethyl) terephthalate (MHET), TPA, and EG. Zhang et al. employed *Taonella mepensis* WT-6 to synthesize bacterial cellulose from PET ammonolysis products (Zhang et al., 2021). During the glycolysis of PET, different catalysts and excess amount of EG are used to break the ester bonds, generating BHET, which can be hydrolyzed and converted to value-added compounds such as protocatechuate, β-ketoadipic acid and glycollate by engineered strains (Kim et al., 2021; Werner et al., 2021). These studies demonstrated the great potential for bioconversion of the PET hydrolysates to higher-value chemicals.

Recently, many efforts have been done to improve the activity and stability of PET hydrolases (Kawai, Fusako, 2021; Kawai, F., 2021; Zhu et al., 2022). The protein variants derived from PET hydrolases such as *Thermobifida fusca* cutinase (Tfcut2) (Li et al., 2022; Then et al., 2015; Then et al., 2016), leaf-branch compost cutinase (LCC) (Tournier et al., 2020) and *Ideonella sakaiensis* PETase (Cui, Y. et al., 2021; Yoshida et al., 2016) benefit from improved thermostability and activity, making enzymatic hydrolysis of PET more efficient and applicable. The most promising variant LCC^{ICCG}

Electronic copy available at: https://ssrn.com/abstract=4110033

can efficiently hydrolyze PET with the TPA productivity up to 16.7 g L^{-1} h^{-1} at 72 °C, providing the possibility to create a fully biological process for PET recycling. Sadler et al. used semi-purified LCC from *E. coli* BL21(DE3) to hydrolyze PET, and the hydrolysates were then converted to vanillin by whole cell catalysis with another engineered *E. coli* RARE_pVanX (Sadler and Wallace, 2021). Similarly, Tiso et al. used the purified LCC to hydrolyze PET and then converted the hydrolysates to PHA by *Pseudomonas umsongensis* GO16 (Tiso et al., 2021). In our previous study, we have proposed a co-cultivation system using the engineered *Yarrowia lipolytica* and *Pseudomonas stutzeri* to achieve the coupling of PET degradation and polyhydroxybutyrate (PHB) production (Liu et al., 2021a). However, due to the low efficiency of PETase, it was only able to convert the BHET but not PET into PHB at that time (Liu et al., 2021a).

Muconic acid (MA) is an important unsaturated dicarboxylic acid, which can be used to produce commodity, new functional resins, pharmaceuticals and agrochemicals (Yoshikawa et al., 1990). Studies have demonstrated MA production from aromatic compounds by directing carbon flux to catechol(Xie et al., 2014). The aromatic compound TPA from PET hydrolysate can also be converted to catechol via protocatechuate and as an example for upcycling, is highly suitable for the biosynthesis

Electronic copy available at: https://ssrn.com/abstract=4110033

of MA (Kim et al., 2019). In this study, we designed a sustainable and circular bioprocess (Fig 1) that continuously convert PET to MA using an engineered multifunctional *P. putida* KT2440 that can simultaneously secrete LCC and metabolize PET monomers. PET was first enzymatically hydrolyzed to produce TPA and EG employing the LCC crude enzyme from culture supernatant. Subsequently, TPA was converted to MA in the next round of fermentation and another hydrolysate EG was used to support cell growth. MA and LCC in the culture supernatant can be separated by ultrafiltration. The reproduced LCC can continue to hydrolyze PET and start a new cycle, allowing continuous production of MA from PET.

2. Materials and methods

2.1. Strains and cultivation

E. coli DH5α used for plasmids construction and clone was cultivated in LB (10 g/L tryptone, 5 g/L yeast extract, and 10 g/L NaCl) at 37 °C and 220 rpm. Primary and conventional cultivation of *P. putida* KT2440 and derived strains was performed in LB at 30 °C and 220 rpm. Mineral medium (MM) used in this study contains 34.74 g/L $Na_2HPO_4 \cdot 12H_2O$, 0.408 g/L KH_2PO_4, 2 g/L NH_4Cl, 1 g/L NaCl, 2 mM $MgSO_4$, 0.1 mM $CaCl_2$ and 1 mL/L trace element solution (TES). TES contains 50 g/L Na_2EDTA, 20 g/L $ZnSO_4 \cdot 7H_2O$, 5.5 g/L $CaCl_2$, 5 g/L $MnCl_2 \cdot 4H_2O$, 1.0 g/L $(NH_4)_6Mo_7O_{24} \cdot 4H_2O$,

Electronic copy available at: https://ssrn.com/abstract=4110033

104 5.0 g/L $FeSO_4 \cdot 7H_2O$, $CuSO_4 \cdot 5H_2O$ 1.5 g/L, 1.61 g/L $CoCl_2 \cdot 5H_2O$. The fermentation
105 was performed in MM or LB with simulated or actual PET hydrolysates. Glucose was
106 appropriately added as a carbon source during the cultivation process to support the
107 growth. If necessary, kanamycin antibiotic was added as the working concentration of
108 25 mg/L. The content of agar in the solid medium was 20%.

109 **2.2. Plasmid construction and strain engineering**

110 Codon-optimized *aro*Y (GenBank: ADF61496), *ecd*B (GenBank: ADF63617)
111 (Johnson et al., 2016) and LCC^{ICCG} (hereafter referred to as LCC)(Tournier et al., 2020)
112 genes were synthesized by GeneralBio, China. The *tph* operon genes *tph*R (GenBank:
113 QTF59206), *tph*A1 (GenBank: QTF59202), *tph*A2 (GenBank: QTF59205), *tph*A3
114 (GenBank: QTF59204), *tph*B (GenBank: QTF59203) and *tpa*K (GenBank: QTF59201)
115 were cloned from a TPA degrading *P. stutzeri* isolated from PET waste in our previous
116 study (Liu et al., 2021b). Polymerase chain reaction (PCR) was performed with Phanta
117 Max Super-Fidelity DNA Polymerase (Vazyme). Oligonucleotides used in this study
118 were synthesized by TsingKe, China and shown in Table S1. The plasmid backbone
119 and DNA fragments were assembled using MultiF Seamless Assembly Mix (ABclonal)
120 according to the manufacturer's instructions. The assembled products were directly
121 transformed into *E. coli* DH5α chemically competent cell (TsingKe, China) for plasmid

Electronic copy available at: https://ssrn.com/abstract=4110033

maintenance. Colony PCR was performed with 2×Taq Plus Master Mix II (Dye Plus) (Vazyme) and plasmid inserts were confirmed with Sanger sequencing performed by TsingKe, China. The genes replacement and deletion of *P. putida* KT2400 were performed via two-step recombination using the vector pK18mobsacB. Initial recombination into the chromosome was selected based on kanamycin resistance gene on LB plates containing 25 mg/L kanamycin, and the second recombination was selected based on sucrose lethal gene (*sac*B) on LB plates containing 20% sucrose. The final correct strains were confirmed by colony PCR and Sanger sequencing. The detailed information of plasmids and strains was shown in Table 1.

Table 1

Strains and plasmids used in this study.

Strains and plasmids	Relevant properties	Sources
pK18mobsacB	Allelic exchange vector, *ori*ColE1 Mob^+, *sac*B, Km^r	Lab Stock(Yu et al., 2015)
pBBR1MCS-2	Protein expression vector, pBBR1 replicon, Mob^+, Km^r	Lab Stock(Zhang et al., 2018)
pBBR-LCC	LCC expression driven by IPTG-induced lac promoter on pBBR1MCS-2	This study

Electronic copy available at: https://ssrn.com/abstract=4110033

E. coli DH5α	F– φ80lacZΔM15 Δ(*lac*ZYA-argF)U169 *deo*R *rec*A1 *end*A1 *hsd*R17(rK–, mK+) *pho*A *sup*E44 λ– *thi*-1 *gyr*A96 *rel*A1 , used for plasmids construction and clone.	Lab Stock
P. putida KT2440	Wild-type	Lab Stock
P. putida KT2440-t	*P. putida* KT2440 (Δ*pca*HG::*tph*), genomic replacement of *pca*HG with tph cluster (*tph*RA2A3A1BK).	This study
P. putida KT2440-ta	*P. putida* KT2440 (Δ*pca*HG::*tph*::*aro*Y:*ecd*B), additional insertion of codon-optimized *aro*Y and *ecd*B follow tph cluster.	This study
P. putida KT2440-tac	*P. putida* KT2440 (Δ*pca*HG::*tph*::*aro*Y:*ecd*B Δ*cat*RBC::Ptac:*cat*A), additional genomic replacement of *cat*RBC with tac promoter, which enabled constitutive expression of *cat*A	This study
P. putida KT2440-tacR	*P. putida* KT2440 (Δ*pca*HG::*tph*::*aro*Y:*ecd*B Δ*cat*RBC::Ptac:*cat*A Δ*gcl*R), additional *gcl*R deletion.	This study

Electronic copy available at: https://ssrn.com/abstract=4110033

P. putida KT2440-tacRD	*P. putida* KT2440 (Δ*pca*HG::*tph*::*aro*Y:*ecd*BΔ*cat*RBC::Ptac:*cat*A Δ*gcl*R::Ptac:*glc*DEF), additional promoter replacement of *glc*DEF wih tac promoter.	This study
P. putida KT2440-tacRDL	*P. putida* KT2440 (Δ*pca*HG::*tph*::*aro*Y:*ecd*BΔ*cat*RBC::Ptac:*cat*A Δ*gcl*R::Ptac:*glc*DEF) (pBBR-LCC), additional LCC expression on pBBR1MCS-2	This study

2.3. Preparation of LCC crude enzyme

P. putida KT2400-tacRDL was inoculated from the overnight cultivated seeds into 50 mL LB containing 25 mg/L kanamycin, and cultivated at 37 °C and 220 rpm for 4 h. And then 0.5 mM isopropyl β-D-1-thiogalactopyranoside (IPTG) was added to induce the expression of LCC for another 20 h. Cells were removed by centrifugation at 12, 000 rpm and the cell free supernatant was filtered with a 10 kDa ultrafilter (Millipore) and concentrated to obtain 1 mL LCC crude enzyme. Cells were disrupted with an automatic sample rapid grinder (Jingxin Technology, China) (Cui, Z. et al., 2021) and analyzed by sodium dodecyl sulfate polyacrylamide gel electrophoresis (SDS-PAGE) as with the cell free supernatant before and after concentration. Total protein concentration of the crude enzyme was determined with the folin phenol reagent

Electronic copy available at: https://ssrn.com/abstract=4110033

(Lowry et al., 1951), and the content of LCC was determined by image analysis using online ImageJ (Alonso Villela et al., 2020) (https://cnij.imjoy.io/).

2.4. Enzyme assays on bis(2-hydroxyethyl) terephthalate (BHET)

BHET particles were purchased from Sigma and the emulsion (4 g/L BHET) was prepared in 100 mM phosphate buffer (34.74 g/L $Na_2HPO_4 \cdot 12H_2O$, 0.408 g/L KH_2PO_4) by ultrasonic pretreatment for 2 min and magnetic stirring for 30 min. For BHET hydrolysis, 300 μL 100 mM phosphate buffer, 200 μL LCC crude enzyme and 500 μL BHET emulsion were mixed and reacted at 40 °C for 1 h. The reaction was stopped by mixed with an equal volume of acetonitrile. The samples were analyzed using high performance liquid chromatography (HPLC) after centrifugation and filtration. Three parallel experiments were carried out in each assay.

2.5. PET enzymatic hydrolysis

Amorphous PET film (Goodfellow) was micronizated under the condition of liquid nitrogen freezing. The particle size of the PET powder was limited to 425 μm by a 35 mesh screen. 0.125 g PET powder and 1 mL LCC crude enzyme prepared from 50 mL culture supernatant was added to 100 mM phosphate buffer (pH 8.0) to a total volume of 10 mL. The catalytic reaction was carried out at 72 °C and 150 rpm in a water bath shaker (Yijing Technology, China). Samples were taken every 12 h and the

Electronic copy available at: https://ssrn.com/abstract=4110033

pH of the reaction system was adjusted to 8.0 with NaOH. The sample was treated with an equal volume of acetonitrile to stop the reaction and analyzed using HPLC after centrifugation and filtration. Two parallel experiments were carried out in each assay.

2.6. Separation of LCC and MA

Cells were removed from the fermentation broth by centrifugation at 12, 000 rpm to obtain the cell free supernatant containing extracellular LCC and MA. LCC and MA were separated by filtration with 10 kDa ultrafilter (Millipore), wherein LCC was in the concentrate and MA was in the exudate. Concentrated LCC crude enzyme was used again for PET hydrolysis. MA was separated and purified from the exudate according to the method reported by Beckham(Vardon et al., 2016). The specific steps include: 1, remove color compounds with 5 wt% activated carbon powder; 2, crystallize at pH 2 and 5 °C. 3, redissolve the crystals in ethanol and filtered to remove insoluble salts. Finally, the recovered MA was dried and determined the purity by HPLC.

2.7. Substrate and product analysis

EG was detected by a refractive index detector using HPLC system equipped with a Bio-Rad Aminex HPX-87H column (7.8×300 mm) as previously (Liu et al., 2021a). Enzymatic hydrolysates including BHET, MHET and TPA were detected by a photodiode array detector at 240 nm using HPLC system equipped with an Agilent

Electronic copy available at: https://ssrn.com/abstract=4110033

ZORBAX Extend-C18 column (4.6×150 mm) as previously (Liu et al., 2021a). Products in the fermentation broth including TPA, protocatechuate, catechol and MA were detected by a photodiode array detector at 230 nm using HPLC system equipped with a longer column Discovery HS C18 (4.6×250 mm). The mobile phase was a solution containing 0.1% (v/v) trifluoroacetic acid and 10% (v/v) acetonitrile. The flow rate and column temperature were set to 0.8 mL/min and 40 °C, respectively.

3. Results and discussion

3.1. Construction of a multifunctional *P. putida* KT2440

To set up a full biological process, a multifunctional host that can degrade PET powder and at the same time convert the degraded TPA and EG to high-value compounds is needed (Fig 1). Muconic acid (MA), which can be applied in the synthesis of new functional resins, pharmaceuticals and agrochemicals was selected as the end product (Kaneko et al., 2011). *P. putida* KT2440, a soil bacterium that can metabolize a variety of aromatic compounds was selected as the host chassis (Ray et al., 2013).

Electronic copy available at: https://ssrn.com/abstract=4110033

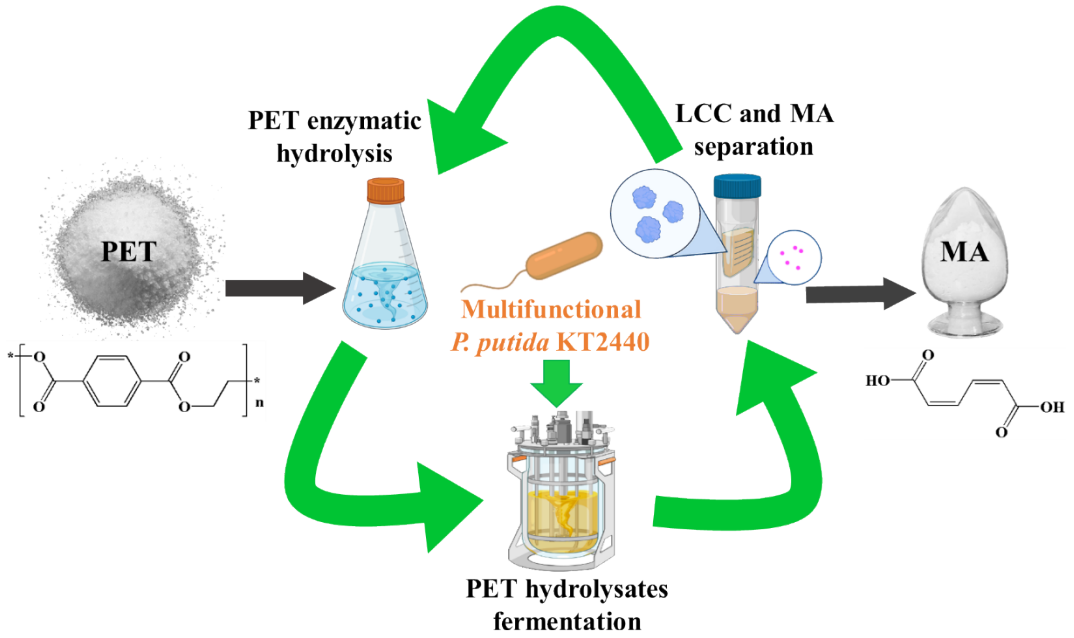

Figure 1. A sustainable circular bioprocess that converts PET to muconic acid (MA) with an engineered multifunctional *Pseudomonas putida*. A leaf-branch compost cutinase (LCC) crude enzyme prepared from the fermentation broth hydrolyzes PET and produces the EG and TPA monomers, which can be directly used as substrates for the following fermentation to produce MA and reproduce LCC. The final product MA can be separated from the LCC crude enzyme by filtration. The remaining concentrated LCC crude enzyme was collected and used for the next round of PET hydrolysis with a stable activity, forming a circular bioprocess.

It has been shown that MA can be produced from lignin-derived aromatic compounds through a pathway involves the intermediates protocatechuate and catechol by *P. putida* KT2440 (Johnson et al., 2016). Whereas protocatechuate is also an intermediate product of TPA metabolism (Sasoh et al., 2006), we presume that MA can

Electronic copy available at: https://ssrn.com/abstract=4110033

be synthesized from TPA via protocatechuate by introducing TPA 1,2-dioxygenase (TphA) and 1,2-dihydroxy-3,5-cyclohexadiene-1,4-dicarboxylate dehydrogenase (TphB) into *P. putida* KT2440 (Fig 2A). In our previous study, we identified a *tph* cluster containing genes encoding the transcriptional regulator (TphR), TPA transporter (TpaK) and TphAB from a TPA degrading *P. stutzeri*, which was isolated from waste (Liu et al., 2021b). To utilize TPA and simultaneously block the metabolic branch of the intermediate protocatechuate in *P. putida* KT2440, we replaced protocatechuate 3,4-dioxygenase encoding genes (*pca*HG) with the *tph* cluster identified in *P. stutzeri.* Then the codon-optimized protocatechuate decarboxylase gene *aro*Y and decarboxylase enhancer gene *ecd*B from *Enterobacter cloacae* was introduced to convert protocatechuate to catechol (Werner et al., 2021). Finally, MA biosynthesis pathway was set up by deletion of the downstream metabolic genes *cat*BC (Salvachúa et al., 2018; Vardon et al., 2015) (Fig 2A).

To prove the function of the host chassis, the engineered *P. putida* KT2440 was cultivated in LB medium containing TPA in a 24-well plate at 30 °C. Samples were took at 24 h for HPLC detection to determine the convertion of substances involved in the mdified metabolic pathway. As expected, TPA was almost not consumed by wild-type *P. putida* KT2440, whereas in *P. putida* KT2440-t expressing *tph* cluster, TPA

Electronic copy available at: https://ssrn.com/abstract=4110033

was almost fully converted to protocatechuate (Fig 2B). After introducing *aro*Y and *ecd*B, protocatechuate was catalyzed into catechol and further metabolized, resulting in a reduction of protocatechuate to 6.4 mM. When the *cat*RBC genes were further replaced with the tac promoter to constitutively express dioxygenase CatA, the resulting strain *P. putida* KT2440-tac produced 4.63 mM MA from 12.86 mM TPA (Fig 2B). In the entire MA pathway, the accumulation of the intermediate product protocatechuate was detected, indicating that protocatechuate decarboxylase activity is the catalytic bottleneck (Curran et al., 2013; Sonoki et al., 2014; Weber et al., 2012). But even so, the final engineered strain *P. putida* KT2440-tac has been able to convert TPA to produce MA.

EG, another hydrolysis product of PET, can be sequentially oxidized to glyoxylate, and then supported the growth of *P. putida* KT2440 via the glyoxylate carboligase (gcl) pathway (Fig 2A) (Franden et al., 2018). However, wild-type *P. putida* KT2440 cannot grow on EG because the *gcl*-operon was repressed by a specific transcriptional regulator (gclR) (Li et al., 2019). To make *P. putida* KT2440 grow on EG, we knocked out *glc*R and overexpressed glycolate oxidase (glcDEF) via the strong, constitutive tac promoter as described by Werner (Werner et al., 2021). The resulting *P. putida*

Electronic copy available at: https://ssrn.com/abstract=4110033

KT2440-tacRD (Δ*pca*HG::*tph*::*aro*Y:*ecd*B Δ*cat*RBC::Ptac:catA Δ*gcl*R::Ptac:*glc*DEF) strain was confirmed to grow on EG (Fig 2C).

To further achieve the functional expression of a PET hydrolase in *P. putida* KT2440-tacRD, LCC was expressed on pBBR1MCS-2 driven by IPTG-induced lac promoter (Fig 2A). We found that the extracellular LCC was comparable whether with and without the native signal peptide (Fig S1). The transfer of LCC from the cytoplasm to the outside of the cell was probably attributed to the activity of phospholipid hydrolyzing, resulting in membrane permeation (Shirke et al., 2018; Su et al., 2013). After optimizing the secretory expression of LCC, the incubation temperature and the inducer concentration of IPTG were determined as 37 °C and 0.5 mM (Fig S2). The 27.8 kDa protein band representing LCC was clearly shown on the SDS-PAGE (Fig 2E). To verify the activity of LCC, culture supernatant was collected to catalyze BHET emulsion hydrolysis at 40 °C as decribed in methods. It was proved by HPLC that BHET was almost completely hydrolyzed to MHET and TPA within 1 h by crude enzyme from *P. putida* KT2440-tacRDL expressing LCC, while enzyme-free phosphate buffer (Control) or the crude enzyme from *P. putida* KT2440-tacRD containing pBBR1MCS-2 without expressing LCC (Empty) can not hydrolyze BHET (Fig 2D).

Electronic copy available at: https://ssrn.com/abstract=4110033

Hereto, *P. putida* KT2440-tacRDL (Δ*pca*HG::*tph*::*aro*Y:*ecd*B Δ*cat*RBC::Ptac:catA Δ*gcl*R Ptac:*glc*DEF) (pBBR-LCC) achieved our expectation, namely secreting PET hydrolase LCC and simultaneous production of MA using PET hydrolysates.

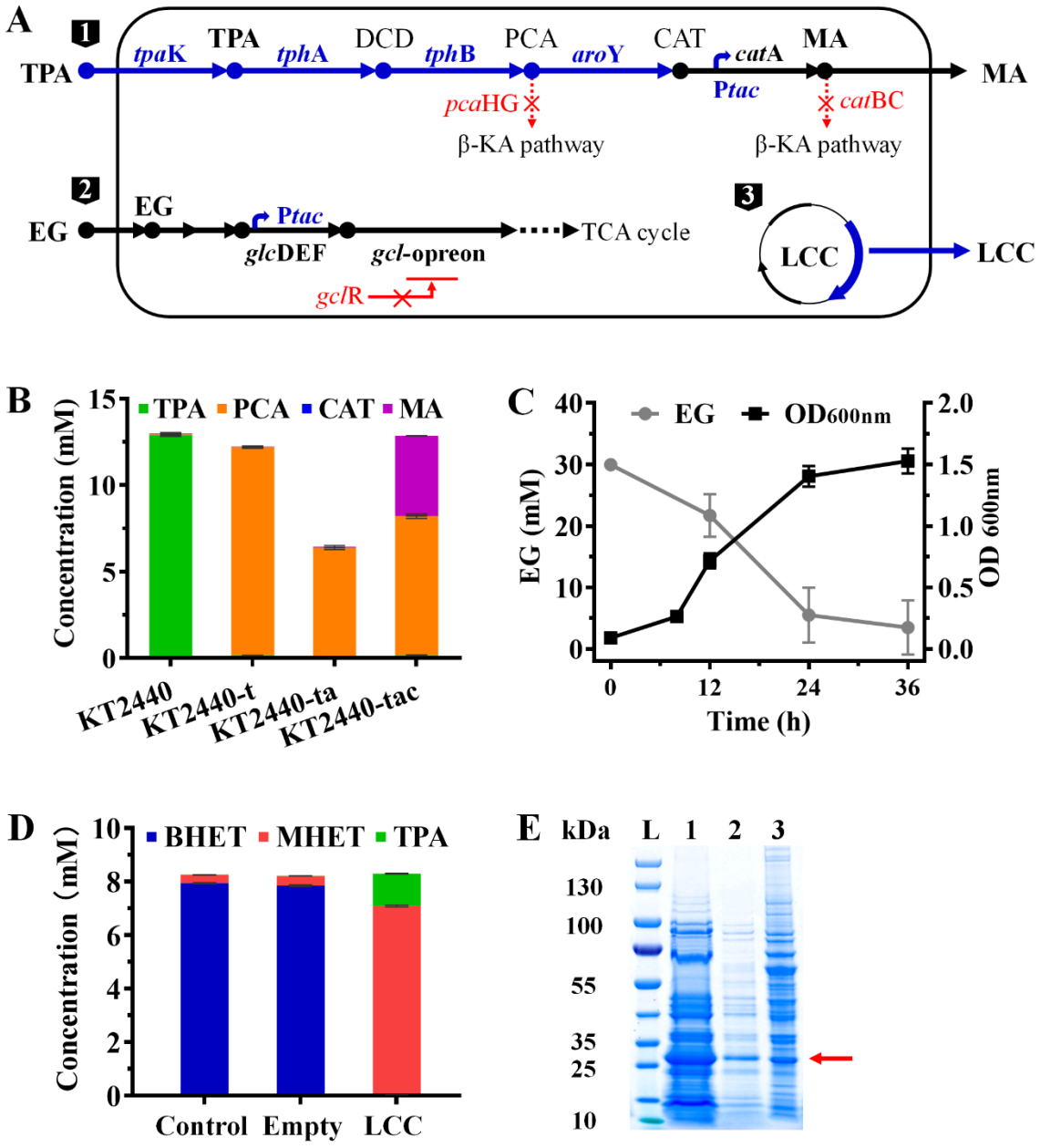

Electronic copy available at: https://ssrn.com/abstract=4110033

Figure 2. Construction of a multifunctional strain. A, *P. putida* KT2440 as the chassis for metabolic engineering design. 1, engineering the metabolic pathway for converting TPA to MA; 2, enhancing the endogenous EG metabolic pathway; 3, secretory expression of LCC on pBBR1MCS-2. B, Bioconversion of TPA by the derived engineered strains in LB containing TPA. KT2440-t refers to the expression of *tph*-operon by replacing *pca*GH in KT2440; KT2440-ta refers to the further expression of *aro*Y-*ecd*B; KT2440-tac refers to the further deletion of *cat*RBC and the promoter replacement of *cat*A with tac promoter. C, Growth and EG metabolism by *P. putida* KT2440-tacRD with the further deletion of *gcl*R and the overexpression of glcDEF. D, BHET hydrolysis by LCC crude enzyme from *P. putida* KT2440-tacRDL. Control refers to enzyme free buffer and empty refers to crude enzyme from strain with an empty vector. E, SDS-PAGE analysis of LCC crude enzyme from *P. putida* KT2440-tacRDL with the further expression of LCC. 1, Concentrated cell free supernatant (10 ×); 2, Cell free supernatant; 3, Cell lysis sample; TPA, terephthalate; DCD, 1,2-dihydroxy-3,5-cyclohexadiene-1,4-dicarboxylate; PCA, protocatechuate; CAT, catechol; MA, muconic acid; EG, ethylene glycol. TpaK, TPA transporter; TphA, TPA 1,2-dioxygenase; TphB, DCD dehydrogenase; AroY, PCA decarboxylase; CatA, CAT 1,2-dioxygenase; glcDEF, glycolate oxidase; *gcl*-operon, genes involved in glyoxylate

Electronic copy available at: https://ssrn.com/abstract=4110033

carboligase metabolic pathway; gclR, the transcriptional regulator that represses the expression of *gcl*-operon; LCC, leaf-branch compost cutinase. Error bars indicate the standard deviation based on triplicate parallels.

3.2. Enzymatic hydrolysis of PET using LCC crude enzyme

50 mL culture supernatant of *P. putida* KT2440-tacRDL was concentrated to 1 mL LCC crude enzyme by filtration with a 10 kDa ultrafilter. The total protein concentration was determined to be 5 mg/mL with the folin phenol reagent (Lowry et al., 1951), and the content of LCC was determined to be 38.70% by image analysis using ImageJ (Alonso Villela et al., 2020) (Fig S3). As a proof, 0.125 g amorphous PET powder and 1 mL LCC crude enzyme (~15 milligrams of LCC per gram of PET) was added to 100 mM phosphate buffer to a total volume of 10 mL. The enzyme was considered to be sufficient relative to the substrate, because it was showed by Tournier that a ratio of 3 milligrams of enzyme per gram of PET appeared to maximize the depolymerization (Tournier et al., 2020). The catalytic reaction was carried out at 72 °C in a water bath shaker. During the hydrolysis of PET, there was little accumulation of BHET with the concentration less than 0.23 mM, while the amount of MHET increased first and then decreased to produce TPA (Fig 3). The TPA productivity over the whole reaction was about 0.15 g L^{-1} h^{-1}, demonstrating the feasibility of directly catalyzing

Electronic copy available at: https://ssrn.com/abstract=4110033

PET hydrolysis using LCC crude enzyme produced by *P. putida* KT2440-tacRDL. However, the hydrolysis efficiency of PET was limited by the small-scale laboratory conditions. It can be further improved by optimizing the concentration of substrate and enzyme as well as finely controlling the pH of the reaction in the large-scale bioreactor system. The reaction was stopped at 48 h as the degradation rate of PET reached 79% and no longer increased (Fig 3). The incomplete degradation may be due to the partial amorphous PET recrystallising at 72 °C during the reaction and no longer be hydrolyzed by the LCC. The final concentration of TPA reached 43.66 mM (Fig 3), that is, at least 0.58 g TPA can be produced from 1 g PET in hydrolysis process catalyzed by LCC crude enzyme produced from *P. putida* KT2440-tacRDL.

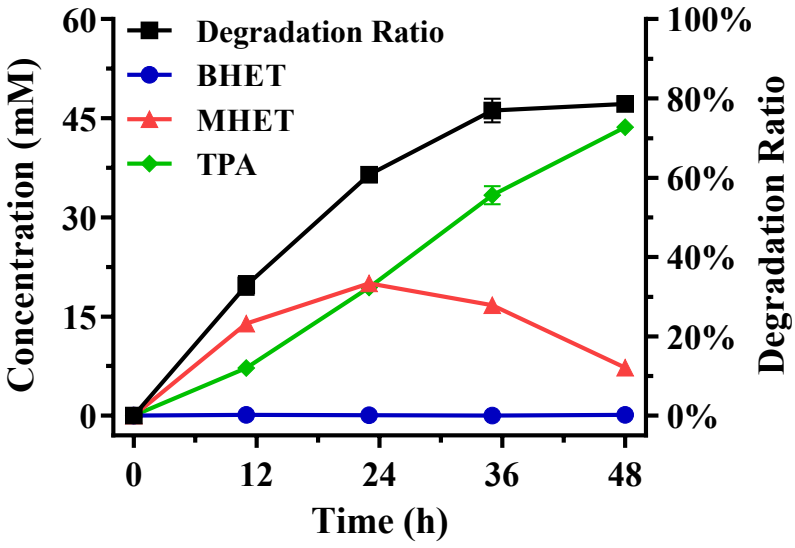

Electronic copy available at: https://ssrn.com/abstract=4110033

Figure 3. PET enzymatic hydrolysis by the LCC crude enzyme produced from *P. putida* KT2440-tacRDL. The data were presented as mean standard deviation of the duplicates.

3.3. Bioconversion of the PET hydrolysates into muconic acid by the engineered multifunctional strain

The bioconversion of muconic acid (MA) was performed by directly mixing the cooled PET hydrolysates with concentrated LB for fermentation by *P. putida* KT2440-tacRDL at 37 ℃. The initial concentration of TPA and EG in the medium were both about 30 mM. The fermentation process lasted for 60 h until TPA was completely converted to MA. The EG was consumed about 11.8 mM (Fig 4). However, when fermented at 30°C, it only required 36 h to completely consume the 18 mM EG (Fig S4A). We believe the main reason is that the optimum growth temperature for *P. putida* KT2440 is at 30 ℃, which is more suitable for the endogenous EG metabolic pathway. Nevertheless, the yield of MA at 30°C was significantly less than that at 37°C, while protocatechuate accumulation increased (Fig S4), suggesting that *aro*Y and *ecd*B derived from *E. cloacae*, which catalyzes protocatechuate convert to catechol, is more active at 37 °C.

Electronic copy available at: https://ssrn.com/abstract=4110033

Therefore, to balance the TPA conversion and EG consumption, the fermentation temperature was determined to be 37 °C. Under this condition, TPA can be converted to MA at molar yield of 100% with almost no intermediate product accumulated, and the productivity of MA reached 0.66 mmol L^{-1} h^{-1} (Fig 4). According to the molecular weight calculation, 0.50 g MA can be produced from per gram PET in one cycle of the bioprocess, reaching 68% of the theoretical conversion. In addition, to reduce the cost, we also evaluated the fermentation in low-cost mineral medium with glucose as a carbon source. Although, the MA productivity in mineral medium was lower than that in LB, TPA can eventually be completely converted to MA at 100% molar yield by extending the fermentation time to 102 h (Fig S5).

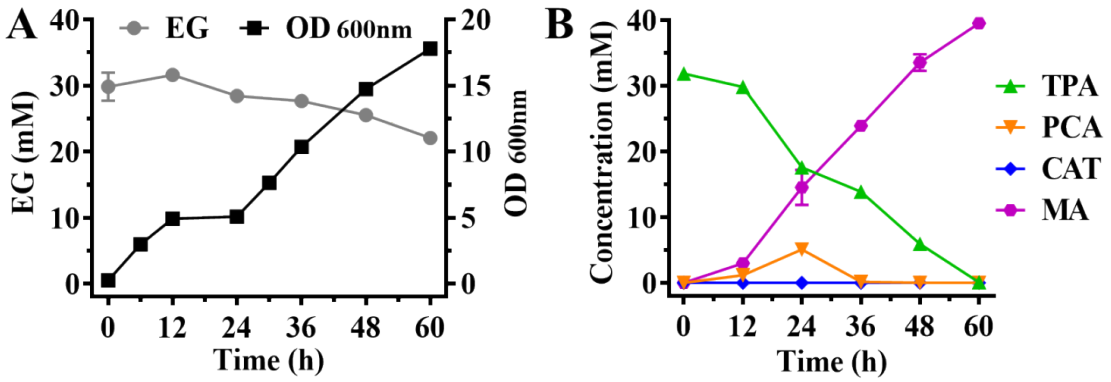

Figure 4. Fermentative production of MA from PET hydrolysates by *P. putida* KT2440-tacRDL. TPA, terephthalate; PCA, protocatechuate; CAT, catechol; MA,

Electronic copy available at: https://ssrn.com/abstract=4110033

muconic acid; EG, ethylene glycol. The data were presented as mean standard deviation of the triplicates.

3.4. Simultaneous separation of MA and preparation of LCC crude enzyme for recirculation

During the fermentative production of MA, PET hydrolase LCC was produced at the same time. Therefore, during the separation of MA, LCC should also be separated. To achieve this purpose, **c**ulture supernatant containing extracellular LCC and MA was collected by centrifugation at 12, 000 rpm to remove cell debris. And then the supernatant was then filtrated with a 10 kDa ultrafilter, wherein LCC was in the concentrate and MA was in the exudate (Fig 5A).

MA was extracted at a recovery of 71.85 % from the exudate by crystallization and purification referencing the reported process (Vardon et al., 2016). In brief, the exudate was first treated with activated carbon powder to remove color compounds. Then, MA was crystallized from the colorless solution at pH 2 and 5 °C. Finally, the MA crystals were dissolved in ethanol and filtered to remove insoluble salts. After drying, MA powder was collected, and the purity was determined by HPLC to be exceeded 99%. (Fig 5B, Table S3).

Electronic copy available at: https://ssrn.com/abstract=4110033

As for PET hydrolase LCC, SDS-PAGE showed a protein band consistent with the size of LCC both in mineral medium (MM) and LB culture, indicating the fermentation using the PET hydrolysate didn't affect the expression of LCC (Fig 5C). Concentrated LCC crude enzyme was used again for PET hydrolysis to recirculate the process. The activity of the collected crude enzyme from 50 mL MM and LB fermentation broth were evaluated for PET hydrolysis, 42.06 mM and 35.30 mM TPA can be produced within 48 h respectively (Fig 5D). In contrast to expressing LCC alone, LCC was also produced in the LB and MM fermentation broth while simultaneously converting PET hydrolysate to MA, and retaining up to 96% and 81% of PET hydrolysis activity, respectively. Moreover, when the reaction lasted for 60 h, there was almost only TPA in the products, which increased to 45.20 mM and 38.26 mM respectively (Fig S6). These results indicated that the yield and activity of LCC crude enzyme during the bioconversion cycle process were stable and can be sustained for recycling and used for PET hydrolysis.

Electronic copy available at: https://ssrn.com/abstract=4110033

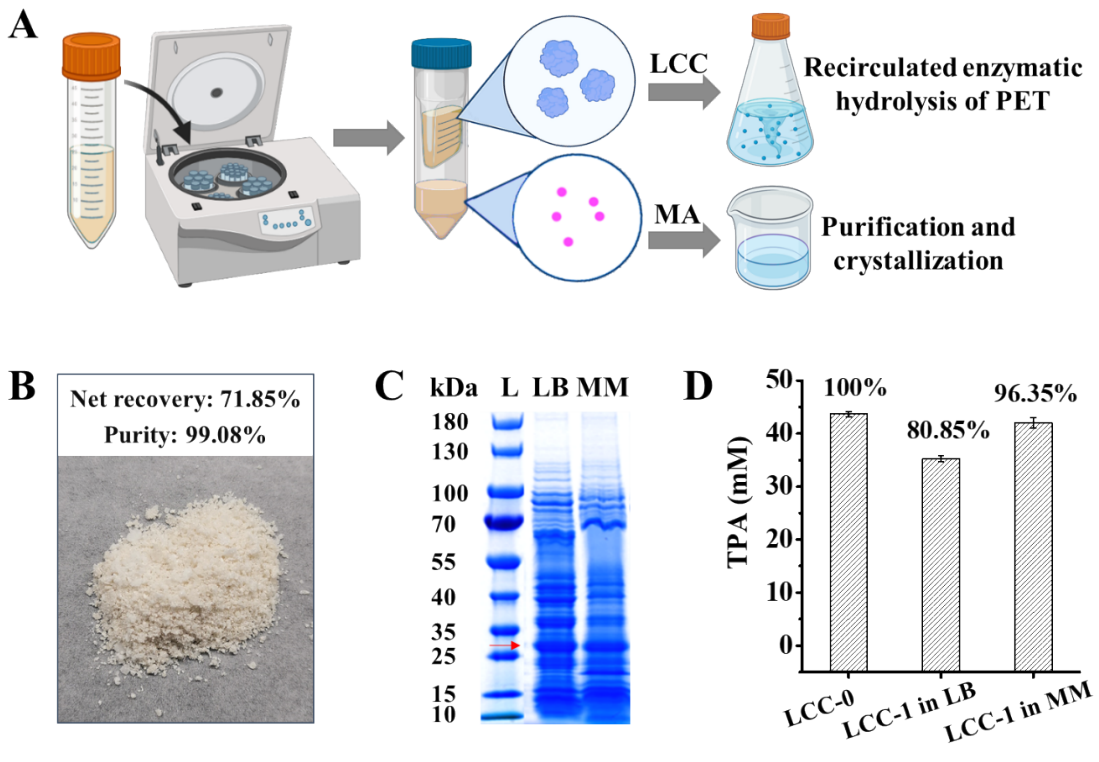

Figure 5. Separation of MA and LCC crude enzyme to validate the circular bioprocess. A, The process for separating the end product MA and the reproduced LCC; B, Recovery rate and purity of the obtained MA powder; C, SDS-PAGE analysis of the crude enzyme from the LB or MM fermentation broth for the conversion of PET hydrolysate to MA. There is a clear thickened band at the size of LCC (approximately 27.8 kDa); D, Activity comparison of LCC crude enzyme form different resources. LCC-0, crude enzyme from LB only expressing LCC; LCC-1 in LB, crude enzyme from LB for the conversion of PET hydrolysate to MA; LCC-1 in MM, crude enzyme from MM for the conversion of PET hydrolysate to MA. Error bars indicate the standard deviation based on duplicate parallels.

Electronic copy available at: https://ssrn.com/abstract=4110033

4. Conclusion

In this study, we designed a sustainable circular bioprocess convert PET to MA. The well-designed multifunctional strain enables continuous hydrolysis of PET and synthesis of the high-value compound MA through a fully circular bioprocess. By optimizing the entire recycling process, we achieved an efficient continuous bioconversion of PET into MA. According to the current process conditions, 0.50 g MA can be produced from per gram PET. Although additional nutritional supplements are required as limited utilization of EG released from PET hydrolysis, the circular bioprocess still reduces the costs compared to conventional two-step processes, in which twice cultivations are needed for the production of PET hydrolase as well as the bioconversion of PET hydrolysates. Future studies will focus on the process optimization including enhancing the metabolic of EG, optimizing the hydrolysis of PET using automated bioreactors and rational time apportioning for PET hydrolysis and fermentation. This process reduces cost and environmental impact, increases sustainability and economic benefits compared to existing conceptually feasible solutions. In conclusion, this study provides a sustainable and circular biological scheme for realizing PET circular economy.

CRediT authorship contribution statement

Electronic copy available at: https://ssrn.com/abstract=4110033

Pan Liu: Investigation, Formal analysis, Resources, Data curation, Writing – original draft, Visualization. **Yi Zheng:** Formal analysis, Visualization. **Yingbo Yuan:** Formal analysis, Visualization. **Tong Zhang**: Investigation, Formal analysis. **Qingbin Li:** Visualization. **Quanfeng Liang:** Supervision. **Tianyuan Su:** Review & Editing, Visualization. **Qingsheng Qi:** Supervision, Funding acquisition.

Declaration of competing interest

The authors declare that they have no known competing financial interests or personal relationships that could have appeared to influence the work reported in this paper.

Acknowledgments

This work was supported by the National Natural Science Foundation of China (grant numbers: 31961133014), and the European Union's Horizon 2020 research and innovation programme under grant agreement No. 870292 (BIOICEP).

References

Alonso Villela, S.M., Kraiem, H., Bouhaouala-Zahar, B., Bideaux, C., Aceves Lara, C.A., Fillaudeau, L., 2020. A protocol for recombinant protein quantification by densitometry. Microbiologyopen 9(6), 1175-1182. https://doi.org/10.1002/mbo3.1027.

Electronic copy available at: https://ssrn.com/abstract=4110033

Barnard, E., Rubio Arias, J.J., Thielemans, W., 2021. Chemolytic depolymerisation of PET: a review. Green Chem. 23(11), 3765-3789. https://doi.org/10.1039/d1gc00887k.

Cui, Y., Chen, Y., Liu, X., Dong, S., Tian, Y.e., Qiao, Y., Mitra, R., Han, J., Li, C., Han, X., Liu, W., Chen, Q., Wei, W., Wang, X., Du, W., Tang, S., Xiang, H., Liu, H., Liang, Y., Houk, K.N., Wu, B., 2021. Computational redesign of a PETase for plastic biodegradation under ambient condition by the GRAPE strategy. ACS Catal. 11(3), 1340-1350. https://doi.org/10.1021/acscatal.0c05126.

Cui, Z., Zheng, H., Jiang, Z., Wang, Z., Hou, J., Wang, Q., Liang, Q., Qi, Q., 2021. Identification and Characterization of the Mitochondrial Replication Origin for Stable and Episomal Expression in Yarrowia lipolytica. ACS Synth Biol. 10(4), 826-835. https://doi.org/10.1021/acssynbio.0c00619.

Curran, K.A., Leavitt, J.M., Karim, A.S., Alper, H.S., 2013. Metabolic engineering of muconic acid production in Saccharomyces cerevisiae. Metab. Eng. 15, 55-66. https://doi.org/10.1016/j.ymben.2012.10.003.

Franden, M.A., Jayakody, L.N., Li, W.J., Wagner, N.J., Cleveland, N.S., Michener, W.E., Hauer, B., Blank, L.M., Wierckx, N., Klebensberger, J., Beckham, G.T., 2018. Engineering Pseudomonas putida KT2440 for efficient ethylene glycol utilization. Metab. Eng. 48, 197-207. https://doi.org/10.1016/j.ymben.2018.06.003.

Electronic copy available at: https://ssrn.com/abstract=4110033

438 Ghasemi, M.H., Neekzad, N., Ajdari, F.B., Kowsari, E., Ramakrishna, S., 2021. Mechanistic
439 aspects of poly(ethylene terephthalate) recycling-toward enabling high quality
440 sustainability decisions in waste management. Environ. Sci. Pollut. Res. 28(32), 43074-
441 43101. https://doi.org/10.1007/s11356-021-14925-z.
442 Ghosal, K., Nayak, C., 2022. Recent advances in chemical recycling of polyethylene
443 terephthalate waste into value added products for sustainable coating solutions – hope vs.
444 hype. Mater Adv. 3(4), 1974-1992. https://doi.org/10.1039/d1ma01112j.
445 Ikenaga, K., Inoue, T., Kusakabe, K., 2016. Hydrolysis of PET by Combining Direct
446 Microwave Heating with High Pressure. Procedia Eng. 148, 314-318.
447 https://doi.org/10.1016/j.proeng.2016.06.442.
448 Johnson, C.W., Salvachua, D., Khanna, P., Smith, H., Peterson, D.J., Beckham, G.T., 2016.
449 Enhancing muconic acid production from glucose and lignin-derived aromatic
450 compounds via increased protocatechuate decarboxylase activity. Metab. Eng. Commun.
451 3, 111-119. https://doi.org/10.1016/j.meteno.2016.04.002.
452 Kaneko, A., Ishii, Y., Kirimura, K., 2011. High-yield Production of *cis,cis*-Muconic Acid
453 from Catechol in Aqueous Solution by Biocatalyst. Chem. Lett. 40(4), 381-383.
454 https://doi.org/10.1246/cl.2011.381.

Electronic copy available at: https://ssrn.com/abstract=4110033

Kawai, F., 2021. The Current State of Research on PET Hydrolyzing Enzymes Available for Biorecycling. Catalysts 11(2), 206. https://doi.org/10.3390/catal11020206.

Kawai, F., 2021. Emerging Strategies in Polyethylene Terephthalate Hydrolase Research for Biorecycling. ChemSusChem 14(19), 4115-4122. https://doi.org/10.1002/cssc.202100740.

Kenny, S.T., Runic, J.N., Kaminsky, W., Woods, T., Babu, R.P., Keely, C.M., Blau, W., O'Connor, K.E., 2008. Up-cycling of PET (polyethylene terephthalate) to the biodegradable plastic PHA (polyhydroxyalkanoate). Environ. Sci. Technol. 42(20), 7696-7701. https://doi.org/10.1021/es801010e.

Kim, D.H., Han, D.O., In Shim, K., Kim, J.K., Pelton, J.G., Ryu, M.H., Joo, J.C., Han, J.W., Kim, H.T., Kim, K.H., 2021. One-Pot Chemo-bioprocess of PET Depolymerization and Recycling Enabled by a Biocompatible Catalyst, Betaine. ACS Catal. 11(7), 3996-4008. https://doi.org/10.1021/acscatal.0c04014.

Kim, H.T., Kim, J.K., Cha, H.G., Kang, M.J., Lee, H.S., Khang, T.U., Yun, E.J., Lee, D.-H., Song, B.K., Park, S.J., Joo, J.C., Kim, K.H., 2019. Biological Valorization of Poly(ethylene terephthalate) Monomers for Upcycling Waste PET. ACS Sustainable Chem. Eng. 7(24), 19396-19406. https://doi.org/10.1021/acssuschemeng.9b03908.

Electronic copy available at: https://ssrn.com/abstract=4110033

Kubowicz, S., Booth, A.M., 2017. Biodegradability of Plastics: Challenges and Misconceptions. Environ. Sci. Technol. 51(21), 12058-12060. https://doi.org/10.1021/acs.est.7b04051.

Li, Q., Zheng, Y., Su, T., Wang, Q., Liang, Q., Zhang, Z., Qi, Q., Tian, J., 2022. Computational design of a cutinase for plastic biodegradation by mining molecular dynamics simulations trajectories. Comput. Struct. Biotechnol. J. 20, 459-470. https://doi.org/10.1016/j.csbj.2021.12.042.

Li, W.J., Jayakody, L.N., Franden, M.A., Wehrmann, M., Daun, T., Hauer, B., Blank, L.M., Beckham, G.T., Klebensberger, J., Wierckx, N., 2019. Laboratory evolution reveals the metabolic and regulatory basis of ethylene glycol metabolism by Pseudomonas putida KT2440. Environ. Microbiol. 21(10), 3669-3682. https://doi.org/10.1111/1462-2920.14703.

Liu, P., Zhang, T., Zheng, Y., Li, Q., Su, T., Qi, Q., 2021a. Potential one-step strategy for PET degradation and PHB biosynthesis through co-cultivation of two engineered microorganisms. Eng. Microbiol. 1, 100003. https://doi.org/10.1016/j.engmic.2021.100003.

Electronic copy available at: https://ssrn.com/abstract=4110033

Liu, P., Zhang, T., Zheng, Y., Li, Q.B., Liang, Q.F., Qi, Q.S., 2021b. Screening and genome analysis of a *Pseudomonas stutzeri* that degrades PET monomer terephthalate. Acta Microbiol. Sin. 62(1), 200-212. https://doi.org/10.13343/j.cnki.wsxb.20210178.

Lowry, O., Rosebrough, N., Farr, A.L., Randall, R., 1951. Protein Measurement with the Folin Phenol Reagent. J. Biol. Chem. 193(1), 265-275. https://doi.org/10.1016/s0021-9258(19)52451-6.

Nikolaivits, E., Pantelic, B., Azeem, M., Taxeidis, G., Babu, R., Topakas, E., Brennan Fournet, M., Nikodinovic-Runic, J., 2021. Progressing Plastics Circularity: A Review of Mechano-Biocatalytic Approaches for Waste Plastic (Re)valorization. Front. Bioeng. Biotechnol. 9, 696040. https://doi.org/10.3389/fbioe.2021.696040.

Qi, X., Yan, W., Cao, Z., Ding, M., Yuan, Y., 2021. Current Advances in the Biodegradation and Bioconversion of Polyethylene Terephthalate. Microorganisms 10(1), 39. https://doi.org/10.3390/microorganisms10010039.

Ray, P., Girard, V., Gault, M., Job, C., Bonneu, M., Mandrand-Berthelot, M.A., Singh, S.S., Job, D., Rodrigue, A., 2013. Pseudomonas putida KT2440 response to nickel or cobalt induced stress by quantitative proteomics. Metallomics 5(1), 68-79. https://doi.org/10.1039/c2mt20147j.

Electronic copy available at: https://ssrn.com/abstract=4110033

505 Sadler, J.C., Wallace, S., 2021. Microbial synthesis of vanillin from waste poly(ethylene
506 terephthalate). Green Chem. 23(13), 4665-4672. https://doi.org/10.1039/d1gc00931a.
507 Salvachúa, D., Johnson, C.W., Singer, C.A., Rohrer, H., Peterson, D.J., Black, B.A., Knapp,
508 A., Beckham, G.T., 2018. Bioprocess development for muconic acid production from
509 aromatic compounds and lignin. Green Chem. 20(21), 5007-5019.
510 https://doi.org/10.1039/c8gc02519c.
511 Sardon, H., Li, Z.C., 2020. Introduction to plastics in a circular economy. Polym. Chem.
512 11(30), 4828-4829. https://doi.org/10.1039/d0py90117b.
513 Sasoh, M., Masai, E., Ishibashi, S., Hara, H., Kamimura, N., Miyauchi, K., Fukuda, M., 2006.
514 Characterization of the terephthalate degradation genes of *Comamonas* sp. strain E6.
515 Appl. Environ. Microbiol. 72(3), 1825-1832. https://doi.org/10.1128/AEM.72.3.1825-
516 1832.2006.
517 Shirke, A.N., White, C., Englaender, J.A., Zwarycz, A., Butterfoss, G.L., Linhardt, R.J.,
518 Gross, R.A., 2018. Stabilizing leaf and branch compost cutinase (LCC) with
519 glycosylation: mechanism and effect on PET hydrolysis. Biochemistry 57(7), 1190-
520 1200. https://doi.org/10.1021/acs.biochem.7b01189.
521 Sonoki, T., Morooka, M., Sakamoto, K., Otsuka, Y., Nakamura, M., Jellison, J., Goodell, B.,
522 2014. Enhancement of protocatechuate decarboxylase activity for the effective

Electronic copy available at: https://ssrn.com/abstract=4110033

production of muconate from lignin-related aromatic compounds. J. Biotechnol. 192, 71-77. https://doi.org/10.1016/j.jbiotec.2014.10.027.

Su, L., Woodard, R.W., Chen, J., Wu, J., 2013. Extracellular location of Thermobifida fusca cutinase expressed in Escherichia coli BL21(DE3) without mediation of a signal peptide. Appl Environ Microbiol 79(14), 4192-4198. https://doi.org/10.1128/AEM.00239-13.

Then, J., Wei, R., Oeser, T., Barth, M., Belisario-Ferrari, M.R., Schmidt, J., Zimmermann, W., 2015. Ca^{2+} and Mg^{2+} binding site engineering increases the degradation of polyethylene terephthalate films by polyester hydrolases from *Thermobifida fusca*. Biotechnol. J. 10(4), 592-598. https://doi.org/10.1002/biot.201400620.

Then, J., Wei, R., Oeser, T., Gerdts, A., Schmidt, J., Barth, M., Zimmermann, W., 2016. A disulfide bridge in the calcium binding site of a polyester hydrolase increases its thermal stability and activity against polyethylene terephthalate. FEBS Open Bio 6(5), 425-432. https://doi.org/10.1002/2211-5463.12053.

Tiso, T., Narancic, T., Wei, R., Pollet, E., Beagan, N., Schroder, K., Honak, A., Jiang, M., Kenny, S.T., Wierckx, N., Perrin, R., Averous, L., Zimmermann, W., O'Connor, K., Blank, L.M., 2021. Towards bio-upcycling of polyethylene terephthalate. Metab. Eng. 66, 167-178. https://doi.org/10.1016/j.ymben.2021.03.011.

Electronic copy available at: https://ssrn.com/abstract=4110033

Tournier, V., Topham, C.M., Gilles, A., David, B., Folgoas, C., Moya-Leclair, E., Kamionka, E., Desrousseaux, M.L., Texier, H., Gavalda, S., Cot, M., Guemard, E., Dalibey, M., Nomme, J., Cioci, G., Barbe, S., Chateau, M., Andre, I., Duquesne, S., Marty, A., 2020. An engineered PET depolymerase to break down and recycle plastic bottles. Nature 580(7802), 216-219. https://doi.org/10.1038/s41586-020-2149-4.

Tsironi, T.N., Chatzidakis, S.M., Stoforos, N.G., 2022. The future of polyethylene terephthalate bottles: Challenges and sustainability. Packag. Technol. Sci. 35(4), 317-325. https://doi.org/https://doi.org/10.1002/pts.2632.

Vardon, D.R., Franden, M.A., Johnson, C.W., Karp, E.M., Guarnieri, M.T., Linger, J.G., Salm, M.J., Strathmann, T.J., Beckham, G.T., 2015. Adipic acid production from lignin. Energy Environ. Sci. 8(2), 617-628. https://doi.org/10.1039/c4ee03230f.

Vardon, D.R., Rorrer, N.A., Salvachúa, D., Settle, A.E., Johnson, C.W., Menart, M.J., Cleveland, N.S., Ciesielski, P.N., Steirer, K.X., Dorgan, J.R., Beckham, G.T., 2016. cis,cis-Muconic acid: separation and catalysis to bio-adipic acid for nylon-6,6 polymerization. Green Chem. 18(11), 3397-3413. https://doi.org/10.1039/c5gc02844b.

Weber, C., Bruckner, C., Weinreb, S., Lehr, C., Essl, C., Boles, E., 2012. Biosynthesis of cis,cis-muconic acid and its aromatic precursors, catechol and protocatechuic acid, from

Electronic copy available at: https://ssrn.com/abstract=4110033

renewable feedstocks by Saccharomyces cerevisiae. Appl. Environ. Microbiol. 78(23), 8421-8430. https://doi.org/10.1128/AEM.01983-12.

Werner, A.Z., Clare, R., Mand, T.D., Pardo, I., Ramirez, K.J., Haugen, S.J., Bratti, F., Dexter, G.N., Elmore, J.R., Huenemann, J.D., Peabody, G.L.t., Johnson, C.W., Rorrer, N.A., Salvachua, D., Guss, A.M., Beckham, G.T., 2021. Tandem chemical deconstruction and biological upcycling of poly(ethylene terephthalate) to beta-ketoadipic acid by Pseudomonas putida KT2440. Metab. Eng. 67, 250-261. https://doi.org/10.1016/j.ymben.2021.07.005.

Xie, N.Z., Liang, H., Huang, R.B., Xu, P., 2014. Biotechnological production of muconic acid: current status and future prospects. Biotechnol Adv 32(3), 615-622. https://doi.org/10.1016/j.biotechadv.2014.04.001.

Xu, S., Zhou, P., Li, H., Juhasz, A., Cui, X., 2021. Leaching and In Vivo Bioavailability of Antimony in PET Bottled Beverages. Environ. Sci. Technol. 55(22), 15227-15235. https://doi.org/10.1021/acs.est.1c02818.

Yoshida, S., Hiraga, K., Takehana, T., Taniguchi, I., Yamaji, H., Maeda, Y., Toyohara, K., Miyamoto, K., Kimura, Y., Oda, K., 2016. A bacterium that degrades and assimilates poly(ethylene terephthalate). Science 351(6278), 1196-1199. https://doi.org/10.1126/science.aad6359.

Electronic copy available at: https://ssrn.com/abstract=4110033

575 Yoshikawa, N., Mizuno, S., Ohta, K., Suzuki, M., 1990. Microbial-Production of Cis,Cis-
576 Muconic Acid. J. Biotechnol. 14(2), 203-210. https://doi.org/Doi 10.1016/0168-
577 1656(90)90009-Z.
578 Yoshioka, T., Grause, G., Eger, C., Kaminsky, W., Okuwaki, A., 2004. Pyrolysis of
579 poly(ethylene terephthalate) in a fluidised bed plant. Polym Degrad Stab. 86(3), 499-504.
580 https://doi.org/10.1016/j.polymdegradstab.2004.06.001.
581 Yu, X., Jin, H., Liu, W., Wang, Q., Qi, Q., 2015. Engineering Corynebacterium glutamicum
582 to produce 5-aminolevulinic acid from glucose. Microb. Cell Fact. 14, 183.
583 https://doi.org/10.1186/s12934-015-0364-8.
584 Zhang, X., Zhang, J., Xu, J., Zhao, Q., Wang, Q., Qi, Q., 2018. Engineering Escherichia coli
585 for efficient coproduction of polyhydroxyalkanoates and 5-aminolevulinic acid. J. Ind.
586 Microbiol. Biotechnol. 45(1), 43-51. https://doi.org/10.1007/s10295-017-1990-4.
587 Zhang, Y., Chen, Y., Cao, G., Ma, X., Zhou, J., Xu, W., 2021. Bacterial cellulose production
588 from terylene ammonia hydrolysate by Taonella mepensis WT-6. Int. J. Biol. Macromol.
589 166, 251-258. https://doi.org/10.1016/j.ijbiomac.2020.10.172.
590 Zhu, B., Wang, D., Wei, N., 2022. Enzyme discovery and engineering for sustainable plastic
591 recycling. Trends Biotechnol. 40(1), 22-37.
592 https://doi.org/10.1016/j.tibtech.2021.02.008.

Electronic copy available at: https://ssrn.com/abstract=4110033

593

Electronic copy available at: https://ssrn.com/abstract=4110033